Angular distribution and spin polarization of Auger-electrons from a potassium (110) surface

1999 J. Phys.: Condens. Matter 11 1861

(http://iopscience.iop.org/0953-8984/11/8/001)

J. Phys.: Condens. Matter **11** (1999) 1861–1872. Printed in the UK PII: S0953-8984(99)98699-X

Angular distribution and spin polarization of Auger-electrons from a potassium (110) surface

Yu Kucherenko† P Rennert‡§ and B Yu Yavorsky†

† Institute of Metal Physics, National Academy of Science of Ukraine, 252142 Kiev, Ukraine
‡ Physics Department, Martin-Luther-University Halle-Wittenberg, D-06099 Halle, Germany

Received 26 October 1998

Abstract. The calculations of the spin-polarized $M_{2,3}VV$ Auger-electron emission following a core-hole excitation by circularly polarized photons from a potassium (110) surface has been performed. The angular distribution of the Auger-electron intensity is discussed and different factors determining the spin polarization of Auger-electrons are examined. It has been shown that the strong angular dependence of the Auger-electron spin polarization, predicted by the atomic model (where only the (ss) two-hole final state is considered), is substantially suppressed by contributions from the p- and d-states in the valence band of potassium crystal. This almost isotropic Auger emission can be significantly modified (particularly with respect to the angular distribution of the intensity) if the diffraction of the outgoing Auger wave on the atoms of the crystal is taken into account. In order to achieve a quantitative agreement of the calculated results with the available experimental data, the theoretical models should be improved to be valid for the accurate treatment of the scattering processes at small kinetic energies of the excited electrons.

1. Introduction

Auger-electron spectroscopy is now a well-recognized method of studying characteristics of the electronic structure of solids [1, 2]. Recently the development of the angle-resolved and spin-resolved spectroscopic techniques has given rise to more detailed investigations of the spatial and energy distribution of the electronic states [3, 4], especially the local magnetic properties of the solids [5, 6]. Spin-polarized Auger-electron spectroscopy has been successfully applied to study ferromagnetic materials [7–10]. However, the spin-polarized Auger emission could also be obtained from non-magnetic materials, if circularly polarized radiation is used for the excitation of the Auger transitions [11–15].

The theoretical study of the spin-polarized Auger-electron emission, excited by circularly polarized radiation from crystal surfaces, has been performed in our preceding works [16–19]. In particular in [19] the K $M_{2,3}VV$ spectra have been considered, and a quantitative agreement with experimental results [14] has been achieved. While, in [14], the experimental data have been published only for the Auger-electron emission within an acceptance cone of $\pm 5^\circ$ around the surface normal, the experimental results are available for different emission directions of Auger-electrons from the potassium (110) surface in [20]. This motivates theoretical studies of the angle-resolved K $M_{2,3}VV$ spectra which aim to analyse the effect of different factors (core-hole polarization, transition matrix elements, Auger-electron diffraction) on the spin-polarized Auger-electron emission.

§ E-mail address: rennert@physik.uni-halle.de.

0953-8984/99/081861+12$19.50

In [21], the first attempt was made to describe theoretically the angular dependence of the spin-polarized Auger spectra from the potassium (110) surface. In spite of a very accurate description of the electron states in the potassium surface layers, performed by means of the full-potential linearized augmented plane wave method, this work gives only a rough picture of the considered Auger process. Firstly, the primary excitation of the core-hole was not studied and, consequently, the orientation and alignment of the core-hole (factors which mostly affect the spin polarization of Auger-electrons) were varied to fit the experimental data. Secondly, only one combination of the valence states involved in the Auger process and only one outgoing partial wave were taken into account. Thirdly, there was no discussion of Auger-electron diffraction processes that could modify considerably the angular distribution of escaping electrons.

In the present work, we have performed the calculations with the aim to overcome shortcomings of [21]. In our theoretical model, we have taken into account the excitation of the core state by circularly polarized light, local valence band structure in K crystal involving all possible valence states in the Auger process and all allowed outgoing partial waves as well as diffraction of the outgoing Auger wave on the atoms of the crystal.

The paper is organized as follows. In the next section, we describe the theoretical model used for calculations. In section 3, we discuss the calculated results for direct (not scattered) Auger waves whose source is a surface atom and an atom in the bulk of the crystal. In section 4, we move to the processes of the Auger-electron diffraction on the surrounding atoms in the crystal. Finally, we give a summary of our results in the last section.

2. Theoretical model

The theoretical model and the main approximations used for the description of the Auger process have been already given in [16, 19].

We assume the CVV Auger process to be a three step process.

(i) An atom in the solid is excited by the incident photon and the core-hole state is created.

(ii) There is Auger decay of the core-hole, which is filled by an electron from the occupied valence band while another valence electron is lifted into an unoccupied state.

(iii) This Auger-electron moves through the crystal to the surface and escapes into the vacuum. On this way it can be scattered at the atoms of the crystal.

We consider the electron states involved in the CVV Auger transition: a core state c (quantum numbers j_c, l_c, μ_c) and two valence states g_1, g_2 (quantum numbers $l_{1,2}, m_{1,2}, \sigma_{1,2}$). The escaping Auger-electron (final state) is described by a sum over spherical waves characterized by quantum numbers $L\ (= l, m)$ and σ.

The spin polarization of the Auger-electrons is expressed in terms of the spin-polarized intensities,

$$P_{\mathrm{AES}} = \frac{I_\uparrow - I_\downarrow}{I_\uparrow + I_\downarrow}. \tag{1}$$

For the considered CVV transition the Auger-electron emission in a direction $\boldsymbol{e}(\boldsymbol{e} = \check{\boldsymbol{k}} = \boldsymbol{r}/r,\ \boldsymbol{k} = k\boldsymbol{e},\ k = \sqrt{E_f})$ can be described by intensities integrated over the energy range of the final Auger-electron states:

$$I_\sigma(\check{\boldsymbol{k}}) = \sum_{g_1 g_2} n_{g_1} n_{g_2} \langle M^2_\sigma \rangle_{g_1 g_2} \tag{2}$$

where n_g is the occupation number for the corresponding valence subband. Auger transition probabilities $\langle M_\sigma^2 \rangle_{g_1 g_2}$ can be expressed as

$$\langle M_\sigma^2 \rangle_{g_1 g_2} = \sum_{\mu_c} w_{\mu_c}(\epsilon, \overline{h}\omega) \left| \sum_L B_{L\sigma}(\boldsymbol{k}) M(L\sigma, c|g_1, g_2) \right|^2 . \tag{3}$$

$w_{\mu_c}(\epsilon, \overline{h}\omega)$ is the photoionization probability for the electron state μ_c in the core shell c. The core-holes μ_c produced in the photoemission process have different weights determined by the dipole transition probability and especially by the polarization of the light. This is a source of the preferred spin orientation of the core shell c. The spin polarization of the hole states is transferred to the Auger-electron via matrix element M of the Auger process:

$$M(L\sigma, c|g_1, g_2) = \langle f_{L\sigma}, c|V|g_1, g_2\rangle - \langle f_{L\sigma}, c|V|g_2, g_1\rangle. \tag{4}$$

It contains the expectation value of the Coulomb interaction and the corresponding exchange integral. $B_{L\sigma}(\boldsymbol{k})$ is the scattering path operator. The same expression describes the electron scattering in LEED and photoelectron diffraction [22–26] and contains the expressions for the direct wave and the multiple scattering contributions and includes the inelastic mean free path. The effect of the electron diffraction on the Auger-electrons depends also on the position $\boldsymbol{R}$ of the atom emitting the Auger-electron in the crystal lattice with respect to the surface. Thus, B depends on $\boldsymbol{R}$ and the Auger intensity is a sum over contributions (2) for different sites $\boldsymbol{R}$. It is assumed that the intensity of the incident light is independent of the position $\boldsymbol{R}$.

As in our preceding work [19], we have considered a geometry similar to the one used in the experiment of Stoppmanns *et al* [14, 20]. Auger-electron emission was excited from the K surface by photoionization with the circularly polarized radiation of positive helicity varying in the energy range 12–24 eV. The experimental data were obtained for the normal incident light. According to this experimental set-up, the axis of quantization chosen in the calculations was parallel to the photon wave vector thus opposite to the surface normal.

We simulate the K(110) surface with a system of muffin-tin potentials. The spherically symmetric potential in the atomic spheres was calculated using the Mattheiss construction [27] which differs for bulk and surface atoms, respectively. For the exchange and correlation part of the potential, the Barth–Hedin approximation [28] was used. The dipole matrix elements and the Auger matrix elements were calculated using scalar-relativistic wave functions. In order to take into account the relaxation processes in the valence band caused by the core-hole (whose life-time is long enough to be screened completely), the Auger matrix elements were obtained using the wave functions, calculated including the core-hole potential whereas, for the dipole matrix elements, the wave functions of the ground state were used. In (2) the occupation numbers $n(g)$ were used which have been obtained for local partial electron states at the atom with a core-hole. They were equal to $n(\mathrm{s}) = 1.062$, $n(\mathrm{p}) = 0.628$ and $n(\mathrm{d}) = 0.278$ [19]. It was assumed that in every l-subband, electrons are uniformly distributed over all m-states.

For the calculations of the Auger-electron diffraction in the crystal we considered a half-spherical cluster, consisting of 251 potassium atoms (scatterers), which was structurally a model for a part of the (110) surface of the bcc crystal. Emitters were arranged in different atomic layers on the symmetry axis of the cluster.

3. Angular distribution of the direct Auger wave

In the first stage of our investigations we consider the direct Auger wave, not taking into account the scattering of outgoing Auger electrons. This gives us the opportunity to analyse our calculated results using theories developed for the angle-resolved Auger-electron emission from free atoms [29–32]. Our consideration differs however from the models for free atoms

because the wave functions for transition matrix elements are obtained in the crystal potential and the screening processes are taken into account. (Note that CVV Auger transition is impossible in the free potassium atom which possesses only one 4s-electron in the valence shell.)

According to the theoretical results presented in [32] the spin polarization of the Auger-electrons for the experimental situation considered in our work can be expressed in terms of the dynamical parameters A_{10}, A_{20}, α, β and γ as

$$P = \frac{I_0 A_{10}}{4\pi I(\theta)}[\beta + \gamma P_2(\cos\theta)] \tag{5}$$

where $P_2(\cos\theta) = \frac{1}{2}(3\cos^2\theta - 1)$ is the Legendre polinomial and

$$I(\theta) = \frac{I_0}{4\pi}[1 + \alpha A_{20} P_2(\cos\theta)] \tag{6}$$

is the angular distribution of the Auger-electrons. Here I_0 is the angle-integrated Auger-electron intensity. The parameters A_{10} and A_{20} determine the polarization state of the ionized atom before the Auger process begins: A_{10} describes the orientation of the core-hole state (i.e.p̃referred μ-state versus $(-\mu)$-state) and A_{20} describes its alignment (i.e.p̃referred $(\pm\mu)$-states as compared with $(\pm\mu')$-states). The parameters α, β and γ depend only on the matrix elements of the Auger decay: α determines the angular distribution of Auger-electrons, β determines the integral (with respect to the angle θ) polarization of the Auger emission and γ determines its differential (angle-resolved) polarization.

In fact the parameters A_{10} and A_{20} depend only on the ratio of the absolute values of the photoionization amplitudes,

$$\lambda = \frac{|D_{l_c-1}|}{|D_{l_c+1}|}. \tag{7}$$

If we consider the excitation of the core p-level the last expression could be reduced to

$$\lambda^2 = \frac{|R_s|^2}{2|R_d|^2} \tag{8}$$

where R_l are the radial parts of the dipol matrix element and the factor 2 arises from the integration over angular parts. For the primary photoexcitation of the core p-level by the circularly polarized photon with positive helicity, the parameters A_{10} and A_{20} are given [32] by the following expressions:

$$A_{10}\left(\frac{1}{2}\right) = -\frac{1}{2}\left(\frac{1-2\lambda^2}{1+\lambda^2}\right) \qquad A_{20}\left(\frac{1}{2}\right) = 0 \tag{9}$$

for the $p_{1/2}$-state, and

$$A_{10}\left(\frac{3}{2}\right) = -\frac{\sqrt{5}}{4}\left(\frac{1-2\lambda^2}{1+\lambda^2}\right) \qquad A_{20}\left(\frac{3}{2}\right) = \frac{1}{20}\left(\frac{1+10\lambda^2}{1+\lambda^2}\right) \tag{10}$$

for the $p_{3/2}$-state.

If the expressions (9) and (10) for A_{10} are compared with formulae for the core-hole spin polarization given in [19], one can see that the values of the parameters A_{10} are proportional but not equal to the core-hole spin polarization. It is important to note that the proportionality coefficients are different for $p_{1/2}$ and for $p_{3/2}$ sublevels ($\frac{1}{3}$ and $-\sqrt{5}/3$, respectively). The same is valid for A_{20}: the alignment of the $p_{3/2}$ hole state is always negative under considered conditions. Thus, the probability to excite states with $\mu = \pm\frac{1}{2}$ is less than that to create holes with $\mu = \pm\frac{3}{2}$ (see table 1 in [19]). However we employ here parameters introduced by Kabachnik and Lee [32] which are widely used to discuss the angular-resolved Auger spectra.

Table 1. Parameters characterizing the polarization state of the potassium atom with the 3p-core-hole excited by circularly polarized radiation (E is the photoelectron energy measured with respect to the Fermi level).

Parameter	$A_{10}\left(\frac{1}{2}\right)$	$A_{10}\left(\frac{3}{2}\right)$	$A_{20}\left(\frac{3}{2}\right)$
Maximal	1.0	1.118	0.5
$E = 0$ eV			
Surface	0.648	0.725	0.394
Bulk	0.597	0.668	0.379
$E = 4.75$ eV			
Surface	−0.441	−0.493	0.068
Bulk	−0.446	−0.499	0.066
Minimal	−0.5	−0.559	0.05

Due to the variation of λ between two extreme values, $\lambda = 0$ (only d-states are allowed for photoelectron) and $\lambda = \infty$ (only s-states are allowed), the parameters A_{10} and A_{20} are changed between their minimal and maximal values that are given in table 1.

By taking into account the actual electronic structure in the potassium crystal in the energy range just above the Fermi level and by performing the calculations of dipol matrix elements for photoexcitation of the 3p-shell, we obtained from (8), for the threshold energy, the values $\lambda^2 = 3.263$ for the surface atom and $\lambda^2 = 2.726$ for the atom in the bulk. As was mentioned above, the excitation of the core level was not treated numerically in [21]. The authors of [21] have only estimated the ratio of probabilities to create the hole with $\mu = -\frac{1}{2}$ and $\mu = -\frac{3}{2}$ in the $3p_{3/2}$ core shell by fitting their calculated results to the experimental data. They obtained the value between $\frac{1}{3}$ and $\frac{2}{3}$. Our calculations give for this ratio (table 1 of [19])

$$\frac{w_{-1/2}}{w_{-3/2}} = \frac{1}{3}\left(1 + \frac{6}{1 + 10\lambda^2}\right) \tag{11}$$

i.e. it changes between the extreme values $\frac{1}{3}$ (for $\lambda = \infty$) and $\frac{7}{3}$ (for $\lambda = 0$). If the photoelectron is excited just above the Fermi level, we obtain for this ratio the value of 0.393 for the surface atom and 0.404 for the atom in the bulk.

For the photoelectron energy of $E = 4.75$ eV (measured with respect to the Fermi level) the values of $\lambda^2 = 0.041$ (surface) and $\lambda^2 = 0.037$ (bulk) are obtained. The photoexcitation process has been already analysed in detail in [19] and it has been shown that just above the 3p threshold there is a considerably larger probability of the transitions into s-states whereas the transitions into d-states dominate at higher energies. The parameters A_{10} and A_{20} calculated for two photoelectron energies are presented in table 1. It should be noted that due to the domination of d-states at $E = 4.75$ eV the values of the parameters are very close to their minimal ones. At $E = 0$ eV the parameters A_{10} and A_{20} reach only about 60% of their maximal value, thus in this case the contribution from photoelectron transitions to d-states may not be neglected in spite of predominant transitions to s-states.

The difference in numeric values calculated for a surface and for a bulk atom can be explained by the difference in potentials for these atoms caused by different atomic surrounding. This gives rise to differences in the wave functions and, consequently, in the matrix elements. These differences are more noticeable at threshold, whereas at higher energies they are not so pronounced. However in all cases the parameter values for a surface atom lie above those for a bulk atom (i.e. deviate towards the maximal value). This reflects the fact that at the surface the unoccupied d-states are shifted to the high-energy side with respect to d-states in the bulk.

From equation (5) and the values of A_{10} given in table 1 it can be seen that the spin

polarization of the Auger-electrons should have different signs for two considered excitation energies. (Due to different signs in A_{10} values, the parameters β and γ are determined only by Auger transition matrix elements and do not depend on the excitation energy.)

In order to obtain the values of parameters α, β and γ, we used the results for the angular distribution of the Auger emission calculated from equations (1)–(4). The angular dependence of the spin polarization of the Auger-electrons for different final states of the emitter are shown in figures 1 and 2. The parameters α, β and γ have been estimated from fitting the curves $P(\theta)$ by the expression (5). The corresponding values are presented in table 2.

Table 2. Parameters characterizing the angular distribution of the M_2VV and M_3VV Auger emission from potassium for different two-hole configurations g_1, g_2.

Final two-hole configuration	M_2VV		M_3VV		
	β	γ	β	γ	α
(ss)	−0.333	1.333	0.745	−0.299	−1.000
(sp)	−0.065	0.535	0.146	−0.119	−0.115
(sd)	−0.153	−0.335	0.339	0.075	+ 0.071
(pp)	−0.091	0.621	0.200	−0.139	−0.118
(pd)	−0.163	0.066	0.363	−0.015	+ 0.086
(dd)	−0.197	0.196	0.440	−0.043	+ 0.059
Total	−0.154	0.054	0.342	−0.012	−0.002

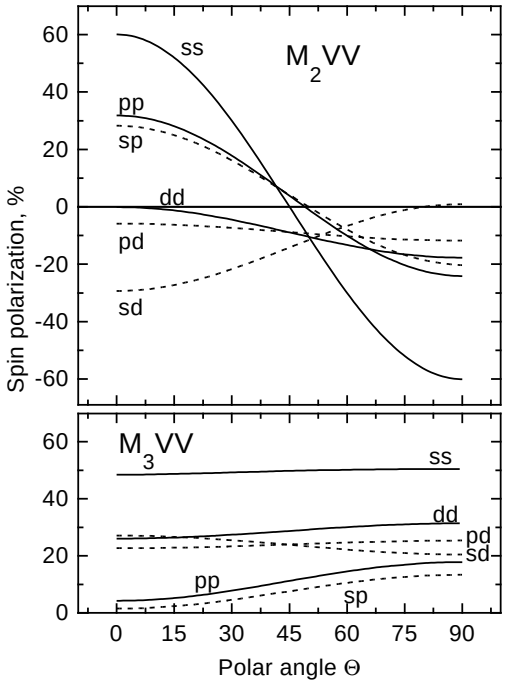

Figure 1. Contributions of different two-hole configurations to the spin polarization of the direct Auger wave for M_2VV and M_3VV transitions versus emission angle. The photoelectron energy is $E = 0$ eV. Results without scattering contributions.

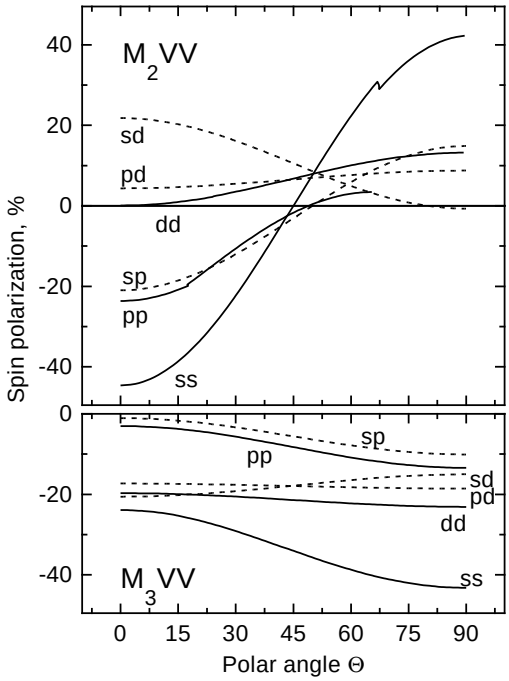

Figure 2. Contributions of different two-hole configurations to the spin polarization of the direct Auger wave for M_2VV and M_3VV transitions versus emission angle. The photoelectron energy is $E = 4.75$ eV. Results without scattering contributions.

In principle, the parameters α, β and γ could be expressed in terms of Auger transition matrix elements and quite clumsy combinations of 6-j and 9-j Wigner symbols [31]. If, however, the selection rules admit only one channel of Auger decay, α, β and γ turn out to be independent of matrix elements and can be immediately evaluated analytically. This is the case for the final (ss) two-hole configuration (only one Auger wave of p-symmetry exists). In [31, 32] the following values can be found for Auger decay of the core p-hole to the singlet S-term: $\beta = -\frac{1}{3}$, $\gamma = \frac{4}{3}$ (for $p_{1/2}$-state) and $\beta = \sqrt{5}/3$, $\gamma = -2/(3\sqrt{5})$, $\alpha = -1$ (for $p_{3/2}$-state). Thus there is a complete agreement with our numerical calculations of the angle-resolved Auger emission (see table 2). Our approach, estimating the parameters by fitting the calculated angular dependences of Auger-electron intensity and spin polarization, also gives the possibility of defining the *effective* values of these parameters for M_2VV and M_3VV spectra, including all decay channels (denoted in table 2 as 'total').

Due to zero alignment of the $3p_{1/2}$ core-hole, the intensity of M_2VV emission is isotropic. As a consequence the angular dependence of the Auger-electron spin polarization changes its behaviour with changing excitation energy in a very simple way. Indeed, according to (5), to obtain the curves of figure 2, we have only to rescale the axis of spin polarization in the corresponding plot of figure 1, employing the ratio of the A_{10} parameters for these two excitation energies. For M_3VV transitions due to anisotropy of Auger-electron intensity, the curves for the angle-dependent spin polarization are modified with changing excitation energy (except for rescaling with the changing sign according to the ratio of the A_{10} parameters). This can be seen if one compares the curves for final (ss) two-hole configuration in figures 1 and 2. This configuration has the maximal anisotropy of intensity (i.e. the maximal value of the parameter α). In this case the Auger wave shows almost isotropic spin polarization for

$E = 0$ eV whereas for $E = 4.75$ eV the spin polarization changes by a factor 2 with increasing polar angle θ. It should be noted however, that the *effective* value of the parameter α for the M_3VV spectrum is very small, i.e. the anisotropy of the Auger-electron intensity is suppressed by Auger decay channels other than the final (ss) two-hole configuration.

It is remarkable that in all considered cases for both M_2VV and M_3VV transitions the contribution from (sd) two-hole configuration to the angle-resolved spin polarization has a converse behaviour as compared to all other contributions: it decreases while the others increase and vice versa. If we take into account that the final (sd) and (pd) configurations provide maximal contributions to the Auger-electron intensity caused by the highest values of the Auger transition probability [19], the total angular dependence of the spin polarization in both M_2VV and M_3VV spectra should be considerably suppressed. It can be seen from table 2 that the *effective* values of the parameter β, which determines the integral spin polarization are close to those for the (sd) and (pd) configurations, whereas the *effective* γ values are small due to opposite sign of the (sd) and (pd) contributions.

Thus, taking account of contributions from the valence p- and d-states causes very weak angular dependence of the Auger-electron spin polarization although Auger transitions to final (ss) two-hole configuration show strong variation of spin polarization with changing polar angle.

4. Auger electron diffraction

It is well known from photoelectron diffraction [33, 34] that electron scattering affects spin polarization. The potassium atoms are non-magnetic scatterers, and the scattering phases are the same for spin-up and spin-down electrons. Thus, for final (ss) two-hole configuration the scattering effects do not appear in the spin polarization. In this case, according to the Auger selection rules, there is only a p-wave outgoing from the emitter, and the diffraction of this wave at the surrounding atoms will not change the ratio of spin-up and spin-down intensities. On the contrary, for other two-hole configurations, there are direct Auger waves of different symmetry (s- and d-waves for (sp) configuration, p- and f-waves for (sd) configuration, s-, d- and g-waves for (pd) configuration, etc) and, consequently, of different partial spin polarization (see table 2 of [19]). The Auger electron diffraction is different for these partial waves and it depends on the position of the scatterer and on the special direction of the Auger emission. Thus, the scattering affects the spin polarization of outgoing Auger electrons, depending on the weight (radial matrix element) of the partial waves. For the final (sp) configuration the intensities of outgoing s- and d-waves differ only by factor 2. Thus, we could expect the Auger-electron scattering to have a significant influence on the spin polarization for the (sp) contribution. However, for all other configurations there is one partial wave that dominates over others (it is, for example, p-wave for (sd) configuration or d-wave for (pd) configuration). As a result, the variations in intensity caused by Auger-electron scattering should affect the resulting spin polarization only slightly.

The theoretical treatment of the Auger-electron diffraction could not be restricted by single-scattering processes because at the considered Auger-electron energies (about 15 eV) the multiple scattering is important. In our calculations we have taken into account the scattering loops up to second order only. Thus, these results could not be expected to be a quantitative description of spin-polarized Auger spectra, but they could give insight into the effects on the Auger-electron spin polarization caused by the scattering processes.

Figure 3 shows the intensity of K $M_{2,3}VV$ Auger-electrons that are emitted from a surface atom and from an atom in the bulk. It can be seen that scattering processes modify considerably the angular distribution of the Auger-electron intensity. Due to the very small value of the

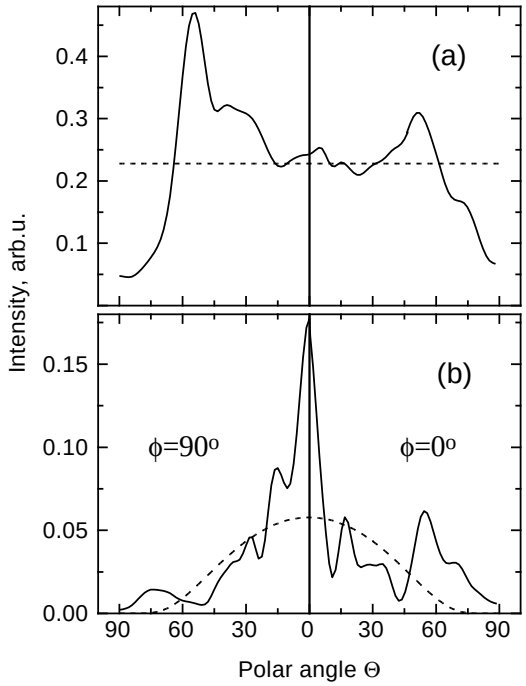

Figure 3. Angular distribution of the K $M_{2,3}VV$ Auger emission from (110) surface: the intensity for electrons emitted from a surface atom (a) and from an atom in the bulk (b). Electron scattering up to second order is included (solid curve) and the contribution of direct (non-scattered) Auger wave is shown (dashed curve).

parameter α (equal to -0.002, see table 2) the direct Auger wave outgoing from the surface atom shows almost isotropic behaviour. The direct Auger wave coming from the bulk (the emitter in the 4th atomic layer was considered) smoothly loses its intensity with increasing polar angle, due to the finite mean free path of electrons in the potassium crystal. Taking account of electron scattering creates the complicated structure in the angle-resolved Auger intensity which is characterized by prominent maxima and minima. Note, that the curve shape is quite different for the surface atom and for the atom in the bulk. The electron scattering tends to enhance the bulk Auger emission normal to the surface whereas the wave emitted from the surface atom is scattered in the surface and subsurface atomic layers giving rise to the maxima at about $\theta = 55^\circ$. The angular distribution of the Auger-electron intensity differs for different azimuthal directions, reflecting the atomic structure near the surface of the crystal.

In figure 4 we have compared our calculations of the Auger-electron spin polarization with the available experimental results [20]. The direct Auger wave shows very weak angular dependence of the spin polarization. For the excitation energy chosen at the $3p_{3/2}$ threshhold it is about 25% and it increases slightly with increasing polar angle θ. If the M_2VV transitions are switched on, the spin polarization has decreasing behaviour and lies between 13 and 14%. The deviations from these values do not exceed 2–3% if the electron scattering is taken into account. Nevertheless the curves are no longer monotone showing maxima and minima at some θ values. For the theoretical results presented in figure 4(a), we could speak about a good agreement with the experimental data (taking account of experimental error). In the case shown in figure 4(b), the calculated and experimental results coincide only for normal Auger emission. For bigger θ values, the experiment provides significantly higher values of

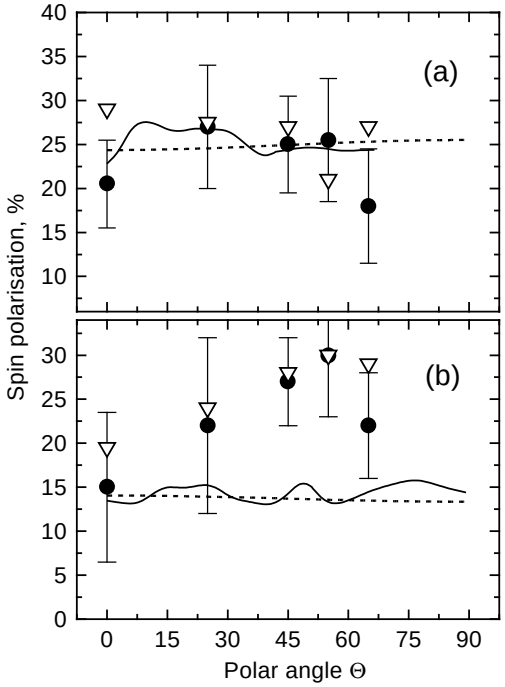

Figure 4. Dependence of the Auger-electron spin polarization on the polar angle if the energy of the initial radiation is (a) at the K $3p_{3/2}$ excitation threshold (M_3VV transitions) and (b) at the K $3p_{1/2}$ excitation threshold (both M_2VV and M_3VV transitions included). Electron scattering up to second order is included (solid curve) and the contribution of direct (non-scattered) Auger wave is shown (dashed curve). Experimental results for K (110) surface (open triangles) and for disordered potassium layers (solid circles) are taken from [20]. Error bars are shown only for latter case.

Auger-electron spin polarization with the maximal value of 30% at $\theta = 55^\circ$. The theoretical results have a maximum at $\theta = 50^\circ$ and it could be expected that the calculated values of the spin polarization will increase for more accurate treatment of scattering processes.

It should be noted that the experimental results obtained for the (110) surface of K crystal and for the disordered sample show no significant differences. For the disordered metallic system we could assume that the short-order arrangement of atoms corresponds to the K bcc structure (or very close to that), but for different emitters the orientation of the surrounding relative to the surface can be different. In this case the correct theoretical approach could be to obtain the result averaged over all possible orientations of the short-order arrangements of atoms. Unfortunately, due to the restricted validity of our theoretical model at low kinetic energies of Auger-electrons this problem could not be treated in detail.

In our calculations the $M_{2,3}VV$ Auger spectrum is considered as a superposition of M_2VV and M_3VV contributions. The experimental data [20] presented in figure 4 are an evidence whether the $3p_{1/2}$ core hole is important for the formation of $M_{2,3}VV$ Auger spectra. Indeed, the values of spin polarization are considerably changed if the excitation energy reaches the $3p_{1/2}$ threshold. Thus, we could not neglect in the calculations the existing $3p_{1/2}$ core hole simply referring to the quick M_2M_3V Coster–Kronig transitions. Either M_2VV transition is not strongly suppressed by the competitive M_2M_3V Coster–Kronig process and contributes to the Auger emission, or the initial state for the M_3VV transition is considerably changed by Coster–Kronig transitions.

5. Conclusions

We have performed the calculations of the angle-resolved K $M_{2,3}$VV spectra taking into account the spin-dependent Auger transition matrix elements, the partial electron state configuration in the valence band and the processes of Auger-electron scattering on the atoms in the crystal. It has been shown that the angular distribution of the Auger-electron spin polarization is determined mostly by the state of the initial core-hole, its orientation and its alignment. All possible Auger decay channels should also be taken into account. A strong angular dependence of the Auger-electron spin polarization, predicted by the atomic model (where only the (ss) two-hole final state is considered), is substantially suppressed by contributions from the p- and d-states in the valence band of potassium crystal. The results are determined mostly by the (sd) and (pd) two-hole configurations due to the biggest values of the Auger transition matrix elements for these contributions.

This almost isotropic Auger emission can be significantly modified (especially the angular distribution of the intensity) by the diffraction of the outgoing Auger wave on the atoms of the crystal. This process should be taken into account for the calculation of the spin-polarized Auger-electron emission, even in the case of non-polarized scatterers in the crystal, if the Auger selection rules allow the outgoing Auger waves with different quantum numbers l. For the chosen direction of the Auger emission the partial contributions to the intensity are changed by the scattering processes as compared to the direct Auger wave, and the value of spin polarization is changed. The scattering processes lead to the non-monotone angular dependence of the spin polarization. In order to achieve a quantitative agreement of the calculated results with the available experimental data the theoretical models should be improved. Multiple scattering beyond second order has to be included and the influence of the M_2M_3V Coster–Kronig process has to be investigated in more detail.

Acknowledgments

We are indebted to Dr N Müller for stimulating discussions. This work was supported by the German Federal Ministry for Education and Research (BMBF) under Grant No. 332-4006-06 HAL 01 (8).

References

[1] Ramaker D E 1991 *Crit. Rev. Solid State and Mater. Sci.* **17** 211
[2] Weightman P 1994 *J. Electron Spectrosc. Relat. Phenom.* **68** 127
[3] Ramaker D E, Fry R A and Idzerda Y U 1995 *J. Electron Spectrosc. Relat. Phenom.* **72** 169
[4] Schneider C M and Kirschner J 1995 *Crit. Rev. Solid State and Mater. Sci.* **20** 179
[5] Kisker E 1985 *Polarized Electrons in Surface Physics* ed R Feder (Singapore: World Scientific) p 513
[6] Landolt M 1985 *Polarized Electrons in Surface Physics* ed R Feder (Singapore: World Scientific) p 385
[7] Sinković B, Johnson P D, Brookes N B, Clarke A and Smith N V 1989 *Phys. Rev. Lett.* **62** 2740
[8] Sinković B, Johnson P D, Brookes N B, Clarke A and Smith N V 1995 *Phys. Rev.* B **52** R6955
[9] Sinković B, Shekel E and Hulbert S L 1995 *Phys. Rev.* B **52** R15703.
[10] Fuchs P, Totland K and Landolt M 1996 *Phys. Rev.* B **53** 9123.
[11] Heinzmann U and Schönhense G 1985 *Polarized Electrons in Surface Physics* ed R Feder (Singapore: World Scientific) p 467
[12] Kuntze R, Salzmann M, Böwering N and Heinzmann U 1993 *Phys. Rev. Lett.* **70** 3716
[13] Stoppmanns P, David R, Müller N and Heinzmann U 1994 *Z. Phys.* D **30** 251
[14] Stoppmanns P, David R, Müller N, Heinzmann U, Grieb H and Noffke J 1994 *J. Phys.: Condens. Matter* **6** 4225
[15] Müller N, David R, Snell G, Kuntze R, Drescher M, Böwering N, Stoppmanns P, Yu S-W, Heinzmann U, Viefhaus J, Hergenhahn U and Becker U 1995 *J. Electron Spectrosc. Relat. Phenom.* **72** 187
[16] Kucherenko Yu and Rennert P 1997 *J. Phys.: Condens. Matter* **9** 5003

[17] Rennert P, Kucherenko Yu and Niebergall L 1998 *J. Magn. Magn. Mater.* **177–181** 1275
[18] Rennert P, Kucherenko Yu and Niebergall L 1998 *J. Electron Spectrosc. Relat. Phenom.* **93** 239
[19] Kucherenko Yu and Rennert P 1998 *Phys. Rev.* B **58** 4173
[20] Stoppmanns P 1995 Spinaufgelöste Auger–Elektronenspektroskopie an metalischen Alkali-Schichten nach Anregung mit zirkular polarisierter Strahlung *PhD Thesis* University of Bielefeld
[21] Jianmin Yuan, Fritsche L and Noffke J 1997 *Phys. Rev.* B **56** 9942
[22] Pendry J B 1974 *Low–Energy Electron Diffraction* (London: Academic Press)
[23] Lee P A and Pendry J B 1975 *Phys. Rev.* B **11** 2795
[24] Fadley C S 1984 *Prog. Surf. Sci.* **16** 275
[25] Rennert P and Chassé A 1987 *Exp. Tech. Phys.* **35** 27
[26] Speder O, Rennert P and Chasseé A 1995 *Surf. Sci.* **331–333** 1383
[27] Mattheiss L F 1964 *Phys. Rev.* **133**A 1399
Mattheiss L F 1964 *Phys. Rev.* **134**A 970
[28] von Barth U and Hedin L 1972 *J. Phys. C: Solid State Phys.* **5** 1629
[29] Klar H 1980 *J. Phys. B: At. Mol. Phys.* **13** 4741
[30] Blum K, Lohmann B and Taute E 1986 *J. Phys. B: At. Mol. Phys.* **19** 3815
[31] Kabachnik N M and Sazhina I P 1984 *J. Phys. B: At. Mol. Phys.* **17** 1335
[32] Kabachnik N M and Lee O V 1989 *J. Phys. B: At. Mol. Opt. Phys.* **22** 2705
[33] Roth Ch, Hillebrecht F U, Park W G, Rose H B and Kisker E 1994 *Phys. Rev. Lett.* **73** 1963
[34] Chassé A and Rennert P 1997 *J. Phys. Chem. Solids* **58** 509